
Article:
Kumar, A. orcid.org/0009-0002-5572-4922, Pandey, V.S. orcid.org/0000-0002-3559-1635, Singh, S. orcid.org/0009-0008-3976-4215 et al. (2 more authors) (2025) High-frequency leaky standing sausage and kink mode waves in magnetic slab. Physics of Plasmas, 32 (7). 072112. ISSN 1070-664X

https://doi.org/10.1063/5.0263251

RESEARCH ARTICLE | JULY 18 2025

High-frequency leaky standing sausage and kink mode waves in magnetic slab

Ankit Kumar ; V. S. Pandey ; Sweta Singh ; Preeti Verma ; R. Erdelyi

Phys. Plasmas 32, 072112 (2025)
https://doi.org/10.1063/5.0263251

High-frequency leaky standing sausage and kink mode waves in magnetic slab

Cite as: Phys. Plasmas **32**, 072112 (2025); doi: 10.1063/5.0263251
Submitted: 4 February 2025 · Accepted: 1 July 2025 ·
Published Online: 18 July 2025

Ankit Kumar,[1] V. S. Pandey,[1,a)] Sweta Singh,[1] Preeti Verma,[2] and R. Erdelyi[3,4,5]

AFFILIATIONS

[1]Department of Applied Sciences, National Institute of Technology Delhi, Delhi 110036, India
[2]Department of Electronics & Communication Engineering, National Institute of Technology Delhi, Delhi 110036, India
[3]Solar Physics and Space Plasma Research Centre (SP2RC), School of Mathematical and Physical Sciences, University of Sheffield, Hicks Bldg, Hounsfield Road, Sheffield S3 7RH, United Kingdom
[4]Department of Astronomy, Eötvös Loránd University, Pázmány P. sétány 1/A, Budapest H-1117, Hungary
[5]Gyula Bay Zoltan Solar Observatory (GSO), Hungarian Solar Physics Foundation (HSPF), Petőfi tér 3., Gyula H-5700, Hungary

[a)]**Author to whom correspondence should be addressed:** vspandey@nitdelhi.ac.in

ABSTRACT

The theoretical framework for analyzing wave and oscillatory behavior in the structured solar corona using slab geometry, where space is filled with uniform low-β plasma, is considered as one of the prominent models for a number of magnetic structures. Numerous observations from the initial findings of the Transition Region and Coronal Explorer satellite to the most recent ones are successfully explained by adopting this model. To formulate the oscillatory characteristics of magnetohydrodynamic (MHD) waves, most studies have the concept of trapped surface and body waves. In this study, we formulate the dispersion relation for leaky fast sausage and kink mode waves to investigate the wave period, damping time, Q-factor, and coronal magneto-seismological characteristics for the non-ideal MHD model by considering a parametric scan of the width and length of the loop. A key aspect of our approach is incorporating viscosity as a damping mechanism, which directly affects the imaginary part of the complex frequency, leading to comparatively more wave damping. In our study, we focus on how viscosity alters the characteristics of leaky fast sausage and kink MHD waves within the low-β regime. The behavior of leaky fast MHD waves is analyzed under the consideration of long ($ka < 1$) and short wavelength ($ka > 1$) approximation of the wave as: (i) For long wavelength limit, the periods of both fast leaky sausage and kink mode waves are influenced solely by the loop width and remain independent of the loop length. However, for the case of short wavelength limit, the period of sausage and kink modes depends on both the loop width and the loop length. (ii) Second, we have studied the impact of non-ideal term (i.e., viscosity) on the damping of these leaky fast MHD waves. The addition of viscosity in the ideal plasma model leads to stronger damping of fast leaky sausage and kink mode waves for both long and short wavelength limits.

I. INTRODUCTION

The study of wave propagation in solar and space plasmas is a fundamental aspect of plasma dynamics. On the one hand, waves play a crucial role in transporting energy across different layers of the solar atmosphere and dissipating this energy in the surrounding region in the form of heat (Einaudi *et al.*, 1993; Erdélyi and Ballai, 2007; Arregui, 2015, Li *et al.*, 2020; and Kolotkov *et al.*, 2020). However, on the other hand, as waves travel through the plasma, they carry with them information about the characteristics of the medium in which they propagate. This latter aspect makes the seismological application of these waves a powerful tool for revealing physical parameters that are otherwise challenging to measure directly, such as magnetic field strengths in the tenuous corona, the magnitude of various transport coefficients, and the intrinsic self-organization of the plasma (Antia, 1986; Gough *et al.*, 1996; Gizon and Birch, 2005; Andries *et al.*, 2009; De Moortel and Nakariakov, 2012; Mathioudakis *et al.*, 2013; and Arregui *et al.*, 2018). Through this solar magneto-seismological (SMS) approach, researchers can gain insights into the otherwise hidden properties of the solar and space plasma environments.

Coronal loop oscillations interpreted as magnetohydrodynamic (MHD) fast kink mode have garnered significant interest since their direct observational detection with the Transition Region and Coronal

Explorer (TRACE) (Aschwanden *et al.*, 1999, 2002; Schrijver *et al.*, 2002) and thereafter by a number of ground-based observations [e.g., the Dunn Solar Telescope (DST), Swedish Solar Telescope (SST), Coronal Multi-channel Polarimeter (CoMP), Goode Solar Telescope (GST), and GREGOR Solar Telescope (GST), as well as space-based missions including the Hinode, Solar Dynamics Observatory (SDO), Interface Region Imaging Spectrograph (IRIS), Solar Orbiter (SolO), and Parker Solar Probe (PSP)]. The theoretical formulation of loop oscillations in leaky mode is already well-developed and initiated, e.g. (Spruit, 1982; Edwin and Roberts, 1983; Cally, 1986; Allcock and Erdélyi, 2017, and Ofman and Wang, 2022), with the latest review by Erdélyi and Zsámberger (2024) and the observation of fast leaky sausage mode waves was reported by Morton *et al.* (2012) in the chromospheric region at a dimensionless wavenumber of approximately $ka \approx 0.08 \pm 0.03$, as shown in their Fig. 4 (also see their supplementary material for more details). Although such waves have not yet been observed in the corona, its existence may not be ruled out and any future observations with high-cadence, space-based instruments may make this possible (Zhong *et al.*, 2023).

The magnetohydrodynamic (MHD) modes in the structured region may be classified into two main categories (trapped and leaky), depending on the consideration of whether wave energy leakage is allowed away from the structure or not. In the magnetic structure, trapped and leaky mode waves follow the inequality condition of $(\alpha_1^2 > 0)$ and $(\alpha_1^2 < 0)$, where the so-called effective wavenumber α_1^2 depends upon the magnitude of ω^2. More details about this will be discussed in Sec. II. Apart from these categorizations, transverse fast MHD waves in a structured region are further classified into kink and sausage mode waves. Sausage modes involve symmetric radial perturbation, where both boundaries of the slab move in phase toward or away from the axis, leading to periodic expansions and contractions of the structure. In contrast, kink modes exhibit asymmetric lateral displacements, where the entire structure oscillates side-to-side with boundaries moving out of phase (Roberts, 2019).

In regard to the trapped fast MHD kink mode, there are various studies that address the transverse oscillations of kink waves and the transfer of energy from transverse to azimuthal directions, leading to damping through the process of mode coupling (e.g., Pascoe *et al.*, 2015; De Moortel *et al.*, 2016; Howson *et al.*, 2020; and Nakariakov *et al.*, 2021). The transverse oscillations of trapped modes in slab geometry were studied and modeled by considering ideal and straight symmetric slab with sharp boundaries (Edwin and Roberts, 1982; Gordon and Hollweg, 1983; Terradas *et al.*, 2005; and Brady *et al.*, 2006), the straight symmetric slab with smooth boundaries (e.g., Edwin and Roberts, 1988; Hornsey *et al.*, 2014; Lopin and Nagorny, 2015; and Yu *et al.*, 2015), the curved magnetic slab (e.g., Verwichte *et al.*, 2006; Díaz *et al.*, 2006; and Lopin, 2022), the straight asymmetric slab with sharp boundaries (e.g., Allcock and Erdélyi, 2017; Chen *et al.*, 2022) and further extended and followed by Porter *et al.* (1994) and Pandey *et al.* (2022a, 2022b) for unstructured and structured atmosphere in the non-ideal plasma. However, for the leaky mode case, specifically, Cally (1986) and later Cally (2003) pointed out that certain solutions of the dispersion relation, known as principal fast leaky modes (PFLK), can decay rapidly. These modes are of interest because they may model the observed damping of transversal loop oscillations. The aforementioned studies primarily address propagating waves; however, our focus here is exclusively on standing mode waves, determining the frequency (ω) by assuming a real and fixed value of k prescribed by the value of loop length. Detailed explanation about standing waves and their boundary conditions is mentioned in Sec. II A.

The physical relevance and the possible role of the fast leaky MHD modes in coronal loop oscillations remain a topic of active debate within the scientific community (Cally, 2006; Ruderman and Roberts, 2006, Goedbloed *et al.*, 2023; and Ebrahimi, 2024). This ongoing discussion highlights the complexity of interpreting these oscillations and the need for further research to fully understand the underlined mechanisms. Understanding the dynamical behavior of the solar corona has depended heavily on the study of leaky mode magnetohydrodynamic (MHD) waves in slab geometry. Leaky modes, also known as pseudo-modes or quasi-normal modes, are characterized by their complex frequencies and pertain to a tendency to dissipate energy away from the region of interest. From the energy point of view, this technique of dissipation of energy is important across the structure. Although leaky modes have been well-documented, their involvement in the eigenvalue problem (EVP) has not received much attention.

Recently, Goedbloed *et al.* (2023) identified three key defects in the standard leaky mode model and proposed solutions to address them. First, discontinuous coefficients in the differential equation, caused by a jump in Alfvén velocity, lead to abrupt changes in the radial wavefunction. To resolve this, they suggested a smoothing procedure to ensure continuity at the boundary. Second, the assumption of "outgoing waves only" beyond a certain point is physically unjustified. Instead, they proposed maintaining boundary continuity, allowing both incoming and outgoing waves for a more accurate representation of wave propagation. Finally, leaky mode solutions exhibit exponential growth at infinity, leading to unphysical energy outflows. They argued that refining the differential equation and excluding such solutions ensure physically meaningful wave behavior. Additionally, a more recent study by Ebrahimi (2024) investigated how both trapped and leaky sausage waves display distinct behaviors influenced by the plasma-beta (β), density ratio, and inhomogeneity parameter.

The defects identified by Goedbloed *et al.* (2023) in the standard leaky mode model are valid, and their corresponding solutions provide crucial insights for improving the model. However, one could adopt a step radial density profile to study leaky mode waves, a concept that is similar to the quantum potential well problem, and also the concept of the antenna theory that radiates energy outside the structure in terms of electromagnetic waves as a result of conversion of guided mode to free space waves. The potential well represents a region, where the Schrödinger wave function is trapped, due to the existence of boundaries defined by potential energy barriers. Depending on the strength of the barrier, whether it is infinite or finite, the wavefunction behavior varies significantly. If the strength of barrier at the boundaries of the well is infinite, the particle associated wavefunction remains almost confined within the structure of the potential well and shows evanescent behavior outside this structure. However, when the strength of the potentials at the boundaries is finite, quantum tunneling/leakage occurs. Therefore, the wavefunction of the wave does not vanish abruptly at the well's boundaries. Instead, the wave shows a propagating behavior outside the structure (Shao *et al.*, 1994; Martín-Palma, 2020). This tunneling effect, associated with resonant states, where the wave is temporarily bound but can eventually leak out, is similar to the

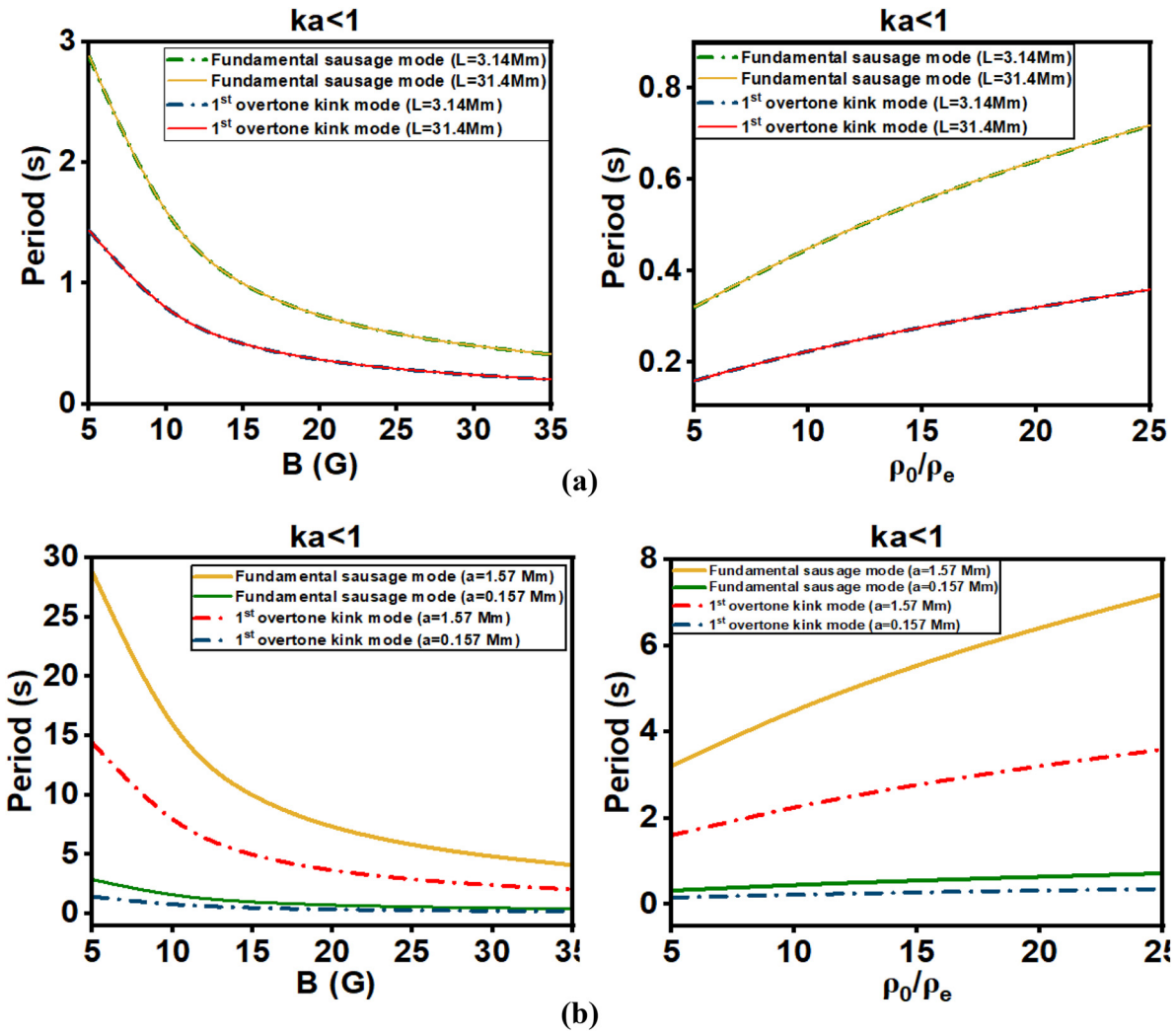

FIG. 4. Variation of period (s) (a) for different length of the loop as a function of magnetic field (G) at $\frac{\rho_0}{\rho_e} = 25$, and as a function of density contrast $\frac{\rho_0}{\rho_e}$ at $B_0 = B_e = 20$ G by keeping the value of radius fixed (i.e., $a = 0.157$ mm) and (b) for different radius of the loop as a function of magnetic field (G) at $\frac{\rho_0}{\rho_e} = 25$, and as a function of density contrast $\frac{\rho_0}{\rho_e}$ at $B_0 = B_e = 20$ G by keeping length of the loop fixed (i.e., $k = 10^{-9}$ cm^{-1}) of leaky fundamental sausage and first overtone kink mode waves at $T_0 = T_e = 10^6$ K, for a different aspect ratio (a/L) of the loop to maintain dimensionless wavenumber, $ka < 1$.

behavior of leaky modes in other physical systems, where confined energy gradually escapes. In principle one can say that this concept is analogous to the behavior of leaky modes in MHD systems. Moreover, the Schrödinger equation that governs the quantum potential well exhibits a similar form of differential equations as represented herein by the governing MHD wave. Thus, the solution of our differential equation (9) is analogous to the quantum approach, and it describes a wave confined or leaking out within a structure is constrained by boundary conditions. This principle of wave dynamics is applied to different domains, whether it is tunneling in quantum mechanics or energy leakage in MHD waves (Sakurai *et al.*, 1986; Griffiths, 1995; and Zettili, 2001). In addition to the above, a similar phenomenon is also observed in antennas, where classical electromagnetic waves are confined within the patch and then leak into the surrounding space (Monticone and Alu, 2015; Zheng *et al.*, 2023; Tofani and Fuscaldo, 2020; and Menon *et al.*, 2023).

In the context of wave leakage, models often exhibit exponential growth of solutions at infinity when the source is continuous and prescribed by driving frequency. However, in our study, we consider an eigenvalue problem (EVP), wherein wavenumber k is prescribed as per the chosen loop length and the evolution of the wavefunction is monitored w.r.t time. This type of input, together with viscosity, leads to damping of waves in the time domain. In other words, one may state that we solve our dispersion relation for estimating the complex frequency by prescribing the wave number k fixed and real valued.

Moreover, researchers have also studied extensively on leaky mode waves for the case of ideal plasma. However, for non-ideal plasma (that includes viscosity, magnetic diffusivity, and thermal

conductivity, as dissipative processes) is still remaining. For non-ideal plasma conditions, in recent study Pandey *et al.* (2022b) analytically examined the effects of viscosity into coronal heating problem through their dispersion relation in a slab model without considering longitudinal perturbations. This study was concerned to the fast trapped mode MHD waves with periods between a second (longer than the ion collision time of about 0.15 s, estimated from Eq. (20) of Kumar and Pandey (2024) to 10 s that are referred to as high-frequency MHD waves, as observed by a number of authors (Williams *et al.*, 2001; Allian and Jain, 2021; and Shrivastav *et al.*, 2024). In contrast to trapped modes, leaky modes leak from the structure and exhibit outwardly propagating fast magnetoacoustic waves. This process is akin to the propagation of electromagnetic waves from a guided structure into free space in antenna theory (Monticone and Alu, 2015; Zheng *et al.*, 2023; Tofani and Fuscaldo, 2020; and Menon *et al.*, 2023). Thus, taking into account the effect of viscosity, this work here is aimed to broaden our knowledge of MHD waves in non-ideal plasmas, particularly concerning the leaky modes. In what follows, we focus on the strength of damping of leaky fast MHD waves with coronal magneto-seismological applications. For the non-ideal plasma model, the value of Q-factor (it determines the number of oscillations before the wave damps into the considering region and defined by ratio of damping time to the wave period) shows stronger damping as compared to the ideal plasma and emphasizes that it depends on the choice of the density contrast ratio and magnetic field strength.

II. THE EQUILIBRIUM MAGNETIC SLAB

In this study, we consider a two-dimensional (2D), static, equilibrium plasma divided into two regions along the x-direction. The equilibrium configuration is depicted in Fig. 1. The central region, referred to as the "slab," has a width of $2a$ in the x-direction and a finite length L in the z-direction. There is no variation in the y-direction $\frac{\partial}{\partial y} = 0$. An equilibrium magnetic field is present, given by $B = B_0\hat{e_z}$, where,

$$\begin{aligned} B(x) &= B_0 \quad \text{if} \quad |x| \le x_0 \\ B(x) &= B_e \quad \text{if} \quad |x| > x_0, \end{aligned} \tag{1}$$

where B_0 and B_e are constants.

The equilibrium kinetic plasma pressure, temperature, and density are denoted by p_i, T_i, and ρ_i, respectively, with $i = 0$ indicating the slab region and $i = e$ representing the external region. For simplicity, gravitational effects are neglected throughout this analysis.

A. The boundary conditions

Boundary conditions are applied at the interfaces $x = \pm a$ and at the slab endpoints $z = 0, L$, where line-tying conditions are imposed. To ensure equilibrium stability, the total pressure balance (p_T) must be maintained across the interface at $x = \pm a$,

$$p_0 + \frac{B_0^2}{2\mu_0} = p_e + \frac{B_e^2}{2\mu_0} = p_T, \tag{2}$$

where μ_0 represents the permeability of free space. The sound speed, denoted as c_i, is given by $c_i = \sqrt{\frac{\gamma p_i}{\rho_i}}$ for $i = o, e$, where γ is the adiabatic index. This index is assumed to be constant across the entire system under the assumption of uniform plasma composition. The line-tying assumption enforces specific boundary conditions at $z = 0, L$: the x-component of the velocity perturbation v_x is zero. Furthermore, the total pressure perturbation p_T, defined as the sum of the kinetic plasma pressure perturbation, is also required to be zero at $z = 0, L$. Mathematically, these boundary conditions are expressed as

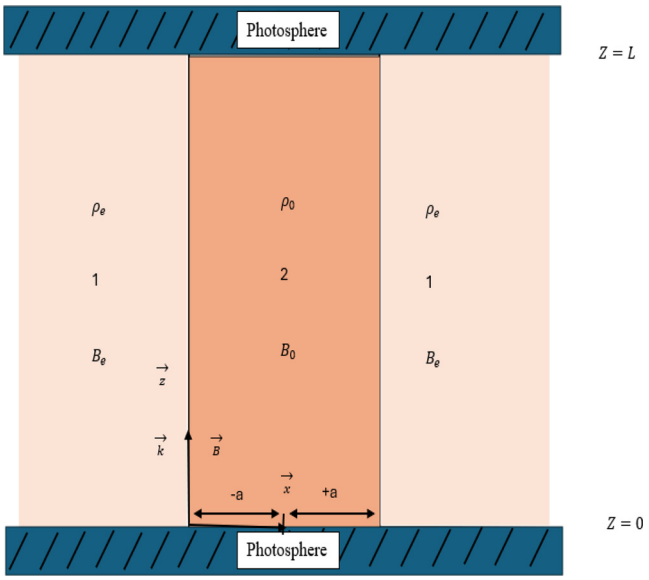

FIG. 1. A schematic diagram of the structured coronal plasma.

$$v_x(z = 0) = v_x(z = L) = 0, \quad p_T(z = 0) = p_T(z = L) = 0. \tag{3}$$

III. GENERAL DISPERSION RELATION

Wave phenomenon (whether propagation or standing one) is commonly studied through its governing dispersion relation, which establishes the relationship between wave frequency and wavenumber, incorporating characteristic speeds and medium-specific parameters. In a structured region, initially, solutions to the governing equations are derived for the plasma regions on both sides of an interface. The dispersion relation is subsequently determined by applying the boundary condition on total pressure and the normal component of velocity, precisely at the boundary interface.

To derive the general dispersion relation, we have considered a comprehensive set of governing MHD equations for coronal loop plasma conditions, incorporating viscosity as a damping mechanism, which may be written as

$$\frac{\partial \rho}{\partial t} + \nabla \cdot (\rho \mathbf{v}) = 0, \tag{4}$$

$$\rho \frac{D\mathbf{v}}{Dt} = -\nabla p + \frac{(\nabla \times \mathbf{B}) \times \mathbf{B}}{4\pi} - \nabla \cdot \mathbf{II}, \tag{5}$$

$$\frac{\partial \mathbf{B}}{\partial t} = \nabla \times (\mathbf{V} \times \mathbf{B}), \tag{6}$$

$$\frac{Dp}{Dt} + \gamma p\,(\nabla \cdot \mathbf{V}) = (\gamma - 1)\,(\mathrm{Q_{Vis}} - \mathrm{Q_{rad}}). \tag{7}$$

Here, $\mathbf{B}$, ρ, $\mathbf{V}$, p, and γ are the magnetic field, total mass density, velocity, pressure, and ratio of specific heats, respectively. The viscosity tensor in Eq. (5), viscous heating, radiative cooling in Eq. (7), and

convective derivatives are represented by $\prod$, Q_{vis}, Q_{rad}, and $\frac{D}{Dt}$, respectively.

The above equations are valid where viscous heating due to wave perturbation is balanced the radiative losses of the considered region. The expression for viscous heating in covariant form is written as per Eq. (10) of Hollweg (1986)

$$\boldsymbol{Q}_{vis} = 3\mu_0 \left(B^{-2}\, \boldsymbol{B}\cdot\boldsymbol{B}\cdot\nabla \boldsymbol{V} - \frac{\nabla.\boldsymbol{V}}{3} \right)^2, \tag{8}$$

where all the symbols have their usual meanings.

If $\boldsymbol{B}$ is in z-direction, then, the detailed expansion of Eq. (8) corresponds to the second order term of viscous wave heating that is expressed in cartesian coordinate with the compressive viscosity coefficient, μ_0, as Porter *et al.* (1994) and Roberts (2019)

$$\boldsymbol{Q}_{vis} = \frac{\mu_0}{3}\left[\frac{\partial \boldsymbol{V}_x}{\partial x} + \frac{\partial \boldsymbol{V}_y}{\partial y} - 2\frac{\partial \boldsymbol{V}_z}{\partial z} \right]^2. \tag{9}$$

For optically thin plasma, the radiation loss rate can be approximated as described by Bray *et al.* (1991) and Porter *et al.* (1994),

$$\boldsymbol{Q}_{rad} \cong 10^{-18.66}\frac{n^2}{T^{1/2}} \cong 10^{28.9}\frac{\rho^2}{T^{1/2}}\ \mathrm{ergscm^{-3}s^{-1}}, \tag{10}$$

where all the symbols have their usual meanings.

In this study, our main aim is to determine the dispersive characteristics of the viscous MHD waves. Viscosity depends on the viscous stress or the rate of strain tensor, and this relationship is altered with the variation of a magnetic field. In the absence of a magnetic field, the rate of strain tensor is associated with one independent coefficient of viscosity (compressive viscosity, i.e., μ_0). However, in strong magnetic fields, the relationship between the strain tensor becomes more complex due to significant differences in momentum transfer perpendicular and parallel to the magnetic field. This complexity necessitates the use of five distinct viscosity coefficients ($\mu_1, \mu_2, \mu_3, \mu_4, \mu_5$). Out of these five viscosity coefficients, compressive viscosity μ_0 is greater by a factor of $(\Omega_i\, \tau_i)^2$ as compared to shear viscosity ($\mu_0 \gg \mu_1, \mu_2, \mu_3, \mu_4, \mu_5$) in the case of a strong magnetic field. Thus, we can neglect the effect of shear viscosity from the current study. For a detailed study about the viscosity components, authors urge to see original work of Braginskii and Leontovich (1965) and followed by Porter *et al.* (1994), Ofman *et al.* (1994), Erdélyi and Goossens (1995, 1996), Pandey *et al.* (2022b), Russell (2023), and Yu (2023).

To solve the set of Eqs. (4)–(7) in the context of the solar corona, we choose a slab model over the cylindrical one. This is because both geometries show similar dispersive characteristics when the aspect ratio satisfies $ka > 1$ (or $a/L > 0.3$), which is typical for short coronal loops where high-frequency waves (a few to tens of seconds) are observed. Differences appear mainly when $ka \ll 1$, relevant to long loops with wave periods of 100–500 s. Since we focus on high-frequency waves in shorter loops, the choice of geometry becomes less critical. Recent observations (e.g., Morton *et al.*, 2012; Zhong *et al.*, 2023) support the presence of such waves, particularly for leaky sausage modes. Additionally, decoupling transverse and longitudinal perturbations is easier in slab geometry, especially for line-of-sight observations like CoMP (Tomczyk *et al.*, 2007). In cylindrical geometry, this decoupling is mainly limited to sausage modes (m = 0). The slab geometry is also mathematically simpler and allows better control over variations in specific directions. Additionally, extended loops or open field regions with tadpole-like structures are more accurately represented using cartesian coordinates (Verwichte *et al.*, 2005). Taking advantage of the versatility offered by the rectangular slab model and employing Braginskii's (Braginskii and Leontovich, 1965) viscous plasma approach, we applied perturbation theory to the linearize the set of MHD equations around a static state of plasma in order to develop the analytical dispersion relation for MHD waves in slab geometry, such that

$$\begin{aligned} p_0 = p_0(x), \quad \rho_0 = \rho_0(x), \\ \frac{d}{dx}\left(p_0 + \frac{B_0^2}{8\pi} \right) = 0. \end{aligned} \tag{11}$$

It is evident that Q_{vis} is of second order wave heating term and it is to be noted that to maintain the above equilibrium condition, we replace Q_{rad} with $\epsilon^2 Q_{rad}$ in energy equation (7), where $\in$ is the small amplitude wave perturbation parameter. This approach aligns with the methodology used by Porter *et al.* (1994). Since Q_{vis} is also a second-order term, it follows the same argument and can be neglected in the linear regime.

We have examined perturbations of the form $f(x)\exp(ikz)\exp(-i\omega t)$. Here, k represents the wavenumber and ω represents the frequency. By applying this perturbation, we linearized Eqs. (4)–(7) by assuming a low β-plasma condition, wherein plasma pressure is neglected relative to magnetic pressure. Under this assumption, the plasma fluctuations are restricted to be perpendicular to the background magnetic field (assumed to be directed along the z axis). Therefore, the perturbations in the z-direction are significantly smaller when compared to transverse components, i.e., $V_{1z} \ll V_{1x}$ and V_{1y}, throughout the analysis, allowing us to neglect V_{1z} (Porter *et al.*, 1994; Wang, 2011; and Wang *et al.*, 2021) and this process has led us to derive the following differential equation (Pandey *et al.*, 2022b),

$$\frac{d^2 V_{1x}}{dx^2} - \alpha_i^2 V_{1x} = 0, \tag{12}$$

where $\alpha_i^2 = \frac{b_i}{a_i}$ and corresponding to $a_i = c_{Ai}^2 - \frac{i\mu_0\omega}{3\rho_i}$, and $b_i = -\omega^2 + c_{Ai}^2 k^2$. Here, i corresponds to either 0 and e, representing region 2 or region 1 of the structured region, respectively. According to the notation after Eq. (12) for α_i^2 and Fig. 1, the sign of α_2^2 defines the body or surface mode structure inside the slab, whereas the sign of α_1^2 defines the trapped or leaky modes.

Now let us illustrate the solutions of Eq. (12) for a slab model, as shown in Fig. 1, of half-width "a". We isolate region 1 as $|x| > a$, and region 2 as $|x| < a$ with interface at $|x| = a$. We consider density in each region to be constant, such that $\frac{\rho_0}{\rho_e} > 1$.

The corresponding solution of the above equation in different regions can be written as (Porter *et al.*, 1994; Pandey *et al.*, 2022b; Allcock and Erdélyi, 2017; Allcock *et al.*, 2019; and Erdélyi and Zsámberger, 2024)

$$\begin{aligned} V_{1x} &= c_1\ \exp(-\alpha_1\,(x-a)) \quad \text{for} \quad x > a \\ V_{1x} &= c_2\ \exp\ (+\alpha_1\,(x+a)) \quad \text{for} \quad x < -a \\ V_{1x} &= c_3 \cosh\,(\alpha_2\, x) + c_4 \sinh\,(\alpha_2\, x) \quad \text{for}\, |x| < a, \end{aligned} \tag{13}$$

where $\alpha_i^2 = \frac{c_{Ai}^2 k^2 - \omega^2}{c_{Ai}^2 - \frac{i\mu_0\omega}{3\rho_i}}$, and k is the wavenumber, and its further details is mentioned in Eq. (15).

We separate these solutions into sausage and kink modes according to whether c_3 or c_4 equals to zero.

As we know, the general solution for a wave propagating in the z-direction in the slab is written as

$$F(x,z,t) = f(x)\exp i(kz - \omega t), \tag{14}$$

where $f(x)$ describes the amplitude of wave, k represents the wavenumber of the wave along the magnetic field (z-direction), ω represents the frequency of the wave, $F(x,z,t)$ refers to velocity (v) and total pressure (p_T) fluctuations.

For simplicity, we focus on the transverse variation of perturbed quantities w.r.t. z- coordinate variables because it is directly affected by the line-tying condition.

To satisfy the boundary conditions at the foot-points, we impose

$$F(z=0) = 0, \quad \text{and} \quad F(z=L) = 0,$$

which leads to the quantization of wavenumber k, described as below.

The most general solution for a standing wave in the z-direction is given by

$$F(z) = A\sin(kz) + B\cos(kz),$$

where A and B are constants, and k is the longitudinal wavenumber.

Apply Boundary Conditions at $z = 0$,

$$F(0) = A\sin(k.0) + B\cos(k.0).$$

Since $F(0) = 0$, this implies

$$B = 0$$

Thus, the solution simplifies to

$$F(z) = A\sin(kz),$$

Apply Boundary Condition at $z = L$

$$F(L) = A\sin(kL).$$

Since $F(L) = 0$, we must have

$$\sin(kL) = 0.$$

This condition is satisfied if

$$kL = n\pi, \quad n = 1,2,3,\ldots\ldots, \tag{15}$$

where n is the mode number, representing the number of half-wavelengths along the loop.

Thus, the wavenumber k is quantized as

$$F(z) = A\sin\left(\frac{n\pi z}{L}\right), \tag{16}$$

where n determines the standing wave mode:

$n = 1$ (Fundamental Mode): One half-wavelength fits along the loop length L.

$n = 2$ (First Overtone): Two half-wavelengths fit along L.

Higher modes ($n = 3,4,\ldots.$) correspond to additional nodes and antinodes along the loop.

Including the time-dependent part, the full wave solution becomes

$$F(x,z,t) = f(x)\sin\left(\frac{n\pi z}{L}\right)\exp(-i\omega t). \tag{17}$$

The frequency ω is related to the wavenumber k through the dispersion relation of the specific wave mode (e.g., kink or sausage mode).

To satisfy the line-tying condition given below,

$$v_x(z=0) = v_x(z=L) = 0, \quad p_T(z=0) = p_T(z=L) = 0,$$

We assume

$$v_x = \hat{v_x}(x)e^{-i\omega t}\sin kz, \quad p_T = \hat{p_T}(x)e^{-i\omega t}\sin kz.$$

When the line-tying boundary conditions are imposed, meaning $v_x(z=0) = v_x(z=L) = 0$, we obtain a condition on k

$$k = \frac{n\pi}{L}, \quad n \in \mathbb{Z}^+,$$

where $n = 1, 2, \ldots.$ positive integer.

After applying the boundary condition for the total pressure ($p_T(x=-a) = p_T(x=+a)$) and velocity ($v_x(x=-a) = v_x(x=+a)$) across the interface $|x| = a$, we obtain this dispersion relation for sausage and kink mode waves, respectively,

$$\alpha_1 \tanh(\alpha_2 a) + \alpha_2 = 0 \tag{18}$$

and

$$\alpha_1 \coth(\alpha_2 a) + \alpha_2 = 0,$$

or

$$\tanh(\alpha_2 a) = \frac{-\alpha_2}{\alpha_1}, \quad \text{and} \quad \coth(\alpha_2 a) = \frac{-\alpha_2}{\alpha_1}, \tag{19}$$

where $\alpha_i^2 = \frac{c_{Ai}^2 k^2 - \omega^2}{c_{Ai}^2 - \frac{i\mu_0\omega}{3\rho_i}}$.

This dispersion relation is identical to Pandey *et al.* (2022b). Interested readers are encouraged to read the original paper for a thorough, step-by-step derivation of the dispersion relation, that dispersion relation corresponds to the trapped mode ($\alpha_2^2 < 0$, $\alpha_1^2 > 0$). Since, in this paper, we are interested in the leaky mode that requires the different boundary condition ($\alpha_2^2 < 0$, $\alpha_1^2 < 0$). Therefore, the above dispersion relation is now modified using the different values of α_i^2 in Pandey *et al.* (2022b),

$$\tan(\alpha_2 a) = \frac{-\alpha_2}{\alpha_1}, \quad \text{and} \quad \cot(\alpha_2 a) = \frac{-\alpha_2}{\alpha_1}, \tag{20}$$

where $\alpha_i^2 = -\frac{\omega^2 - c_{Ai}^2 k^2}{c_{Ai}^2 - \frac{i\mu_0\omega}{3\rho_i}}$, and, the symbols have their usual meanings.

Furthermore, we have found that excluding the viscosity term from Eq. (20) results in the same dispersion relation as referred in Roberts (2019) and Terradas *et al.* (2005), with the value of α_i^2 modified, for an ideal plasma in the following form:where $\alpha_i^2 = -\frac{\omega^2 - c_{Ai}^2 k^2}{c_{Ai}^2}$, and, again, symbols have their usual meanings.

The dispersion relation (20) is transcendental in nature, which can be solved by numerical techniques. We solve the above said dispersion relation for $\omega(k)$, wherein we assume a fixed value of k and determine ω, corresponding to solutions for standing waves. We calculate the period and damping time from the estimated value of ω. In this

study, we used the *fsolve* function in MATLAB to solve systems of non-linear algebraic equations. It employs various numerical techniques, primarily the trust-region-dogleg, trust-region-reflective, and Levenberg–Marquardt algorithms (Marquardt, 1963; Powell, 1968; Moré, 1977; and Moré *et al.*, 1980). These advanced methods build upon the Newton–Raphson algorithm, enhancing its capabilities to handle a wider range of problems more effectively. To compare our dispersion relation with that of Terradas *et al.* (2005) (where we solved the dispersion relation (20) for complex frequency by specifying the wavenumber k real and fixed which represents a fixed loop length). Thus, we plotted the phase velocity as a function of the dimensionless wavenumber ka as shown in Figs. 2(a) and 2(b) and found that it is consistent with Figs. 1(a) and 1(b) of Terradas *et al.* (2005), where the density contrast is set to 3. The expression $\omega_c = kv_{Ae}$, illustrated by the dotted line in Fig. 1(a), donates the cutoff frequency. Modes below ω_c are classifing as trapped modes, while those above ω_c are classifing as leaky modes.

Unlike Terradas *et al.* (2005), who did not include non-ideal components in their dispersion relation, we incorporated viscosity in our analysis. Despite of this addition, our phase velocity plot remains similar to that of Terradas *et al.* (2005). This is due to the fact that viscosity does not influence the real part of complex frequency, while it alters the imaginary part of the frequency. Hence, the real part, which determines phase velocity, remains unaffected. Figure 2(a) shows the real part of the frequency, ω_r, for the fundamental fast sausage mode and the first kink harmonic. These modes behave as leaky waves when the loop is thin ($a/L < 1$). The frequency curves reach the cutoff frequency ω_c and then split into two branches, as the loop thickness increases with keeping the loop length fixed. This happens near the point where the trapped mode meets the cutoff. One of these branches smoothly connects to the trapped mode, showing a clear link between leaky and trapped solutions. However, the second branch has $\omega_i = 0$, and its eigenfunction grows exponentially with distance from the slab with a non-oscillatory spatial behavior. For this, an initial value analysis is required to verify whether eigenfunction is causal (physical) or not. In such an analysis, such an eigenfunction can appear multiplied by a moving step function representing an outgoing wave front, which is entirely physical.

Figure 2(b) shows the imaginary part of the frequency, ω_i, for the first three leaky modes. For both the fundamental sausage mode and the first kink harmonic, as expected, ω_i becomes smaller and tends to zero as a/L becomes closer to the bifurcation point, where the mode becomes trapped. There is also another solution with a purely imaginary frequency [shown by the solid line in Fig. 2(b)], but since it also grows with distance from the loop, it is not physically meaningful either.

Furthermore, Fig. 3 presents the phase velocity as a function of dimensionless wavenumber ka from our dispersion relation for the leaky region, using a density contrast of 25, because the loops with a density contrast of $\frac{\rho_0}{\rho_e} \geq 20$ exhibit the damping time up to three periods (Farahani *et al.*, 2014). Consequently, the fast sausage and kink mode could be detected for several periods in these high-density contrast loops. The plot clearly shows that the fundamental mode and the first overtone occur when the value of dimensionless wavenumber ka is less than 1 (i.e., $ka < 1$) for both leaky sausage and kink mode waves. Next, when we consider the higher values of dimensionless wavenumber ka, we find higher harmonics that are very challenging to detect. Thus, the wavenumber is a crucial factor in deciding the existence of the leaky waves in plasma, either as fundamental or its first overtone for a given value of density contrast. The phase velocity is only affected when there is change in the real part of the frequency. In this case, it is noted that viscosity only influences the imaginary part (ω_i). Therefore, it does not alter the phase velocity. The phase velocity remains the same for both ideal and non-ideal MHD cases, as a result.

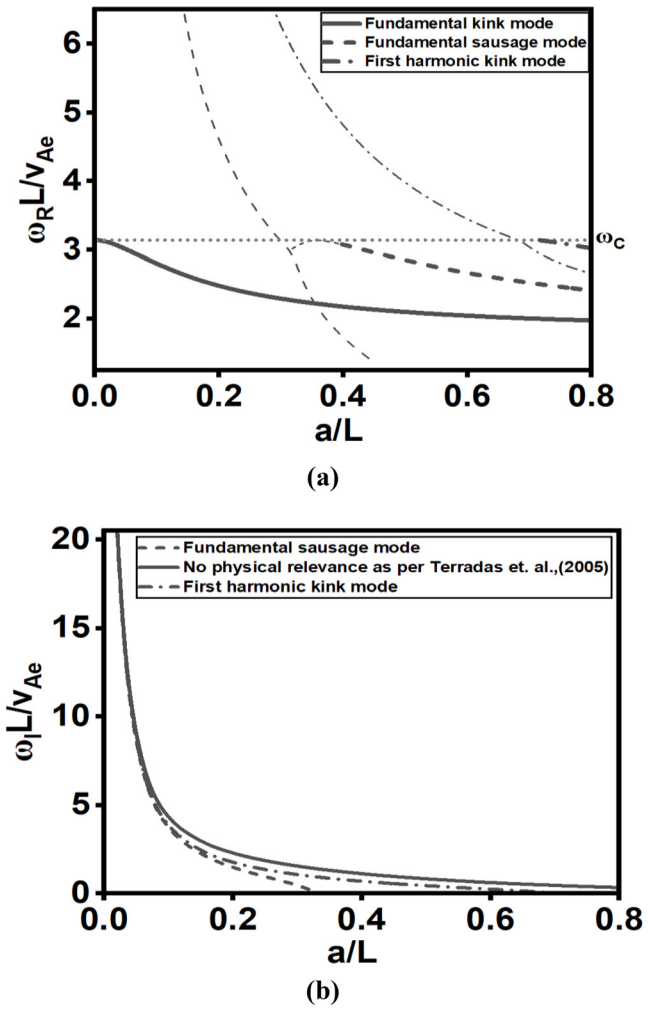

FIG. 2. The plot of dimensionless (a) real frequency and (b) imaginary frequency vs a/L at $T_0 = T_e = 10^6$K, $\frac{\rho_0}{\rho_e} = 3$, $B_0 = B_e = 20$G, $k = 10^{-8}$cm^{-1}. Dashed dotted line represents the kink mode and solid line corresponds to sausage mode. ω_c is the cutoff frequency.

IV. RESULT AND DISCUSSION

Fast MHD leaky mode waves in coronal loops are an intriguing aspect of the solar physics, providing insights into the dynamical processes of the solar corona. These waves are characterized by their ability to transport energy across different regions of the solar atmosphere and dissipate it into the surrounding regions. Leaky mode waves, also known as pseudo-modes or quasi-normal modes, are defined by their complex frequencies even in ideal plasma consideration with the

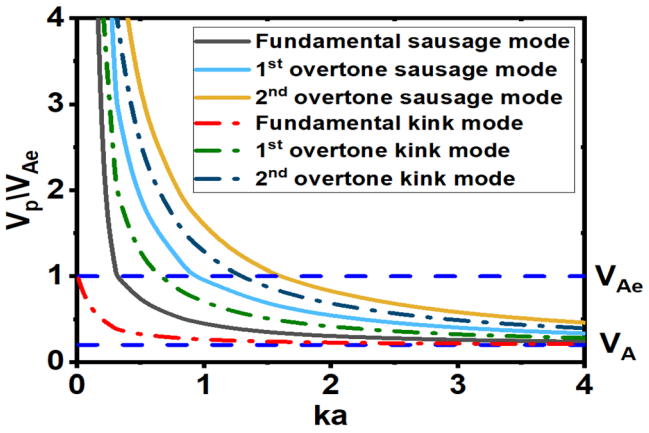

FIG. 3. The normalized phase velocity as a function of dimensionless wavenumber ka at $T_0 = T_e = 10^6$K, $\frac{\rho_0}{\rho_e} = 25$, $B_0 = B_e = 20$G, $k = 10^{-8}$cm^{-1}. Dashed horizontal blue lines correspond to the exterior and interior Alfvén's speeds.

imaginary part indicating energy dissipation. They differ from trapped modes, which have only real frequencies and do not lose energy as they propagate. Leaky modes include both sausage and kink modes, each with distinct oscillatory properties. The behavior of leaky mode waves is heavily influenced by the magnetic field strength and the geometry of the coronal loops. Moreover, the factors such as loop length, width, and density contrast play crucial roles in determining wave periods and damping times.

A. Dependence of wave period on loop width and loop length for both long wavelength (ka<1) and short wavelength (ka>1) approximation

The fast sausage and kink modes exhibit distinctive behaviors with regard to the wave period, damping time, Q-factor, etc., with the variations of magnetic field strength and density contrast, depending on whether $ka < 1$ or $ka > 1$.

B. Case I: For the long wavelength limit (i.e., ka<1)

We present the period profile using our dispersion relation, employing the same parameters and aspect ratio as mentioned in Terradas *et al.* (2005) for $ka < 1$ with a density contrast of 25. Figure 4 shows the periods of fast leaky sausage (fundamental mode) and kink waves (first overtone, as the fundamental mode is cut off in the trapped region) varying with magnetic field strength and density contrast. Adjusting loop width alters the period, while changes in loop length have minimal effect, consistent with Cally (1986) and Roberts (2019). The period decreases with increasing magnetic field strength and increases with higher density contrast, aligning with Roberts (2019, Eq. 5.144). This approach aids solar magneto-seismology, particularly in identifying high-frequency MHD waves (1–10 s periods; Williams *et al.*, 2001; Allian and Jain, 2021; and Shrivastav *et al.*, 2024). For example, a 4-second period for the fundamental sausage mode [Fig. 4(b)] requires a ∼35G magnetic field and a density contrast of ∼7, making this method a valuable tool for coronal diagnostic through wave analysis.

C. Case II: Short wavelength limit (i.e., ka>1)

However, for $ka > 1$, as shown in Fig. 5, the periods of fast leaky sausage (second overtone at $ka = 1.57$) and kink waves (third overtone at $ka = 1.57$) depend on both the loop width and length, which is similar to the pattern of Fig. 4. These results are consistent with Roberts (2019, Eqs. 5.124 and 5.135), emphasizing the role of magnetic field, density contrast, and loop geometry in coronal plasma dynamics. Like case I, the case II also holds significance for coronal magneto-seismology. So far, our analysis concerning the fast leaky MHD waves was based on without considering the effect of viscosity. Now, in Sec. IV D, we are analyzing the effect of viscosity on the characteristics of fast leaky modes.

D. Effect of viscosity on the fast leaky sausage and kink mode for the case of ka<1 and ka>1

We have investigated the effect of viscosity on the fast leaky fundamental sausage and first overtone kink mode waves (the higher harmonics have not been taken into consideration since there is no such observation so far) for both long ($ka < 1$) and short ($ka > 1$) wavelength limits as calculated in Figs. 4 and 5. In the case of leaky modes, the frequency ($\omega = \omega_r - i\omega_i$) consists of real and imaginary components, for both ideal and non-ideal plasma. The imaginary component is responsible for wave damping. It is noted that the viscosity term modifies the imaginary part of the complex frequency significantly, thus affecting wave damping. To demonstrate this, we have plotted the damping time profile as a function of the magnetic field in Figs. 6(a) and 6(b) for the fast leaky fundamental sausage and first overtone kink mode waves for the different values of aspect ratio (a/L) of the loops. When the loop width is decreased while keeping the loop length constant, or vice versa, the ratio of a/L decreases, resulting in a thinner and longer loop that exhibits stronger damping compared to a wider and shorter loop. Damping time profile decreases with increasing magnetic field as shown in Figs. 6(a) and 6(b) for both ideal and non-ideal plasma. The quantitative percentage variation in damping time due to viscosity for fast sausage and kink mode waves, in both the short- and long-wavelength regimes, illustrated in Figs. 6(c) and 6(d), is calculated using Eq. (21). Specifically, for the leaky sausage mode in Fig. 6(c), the long-wavelength limit exhibits approximately 14% greater damping w.r.t ideal plasma at lower value of magnetic field strengths, which gradually decreases to about 2% as the magnetic field increases. In the short-wavelength regime, this variation is more pronounced, reaching up to 64% at lower magnetic fields and similarly reducing to around 20% at higher values of magnetic field strength. For the fast leaky kink mode shown in Fig. 6(d), the damping time in the long-wavelength regime varies from roughly 37% to 5% as the magnetic field increases from 5G to 35G. In the short-wavelength regime, the variation ranges from approximately 47% to 12% over the same range of magnetic field strength.

In all cases, the influence of viscosity on damping time decreases with increasing magnetic field strength. These findings suggest that long-wavelength leaky waves contribute more significantly to both coronal heating and magneto-seismology than their short-wavelength counterparts. Understanding this distinction is crucial for determining which wave modes are more efficient in dissipating energy in the solar corona and for enhancing the diagnostic capability of coronal magneto-seismology.

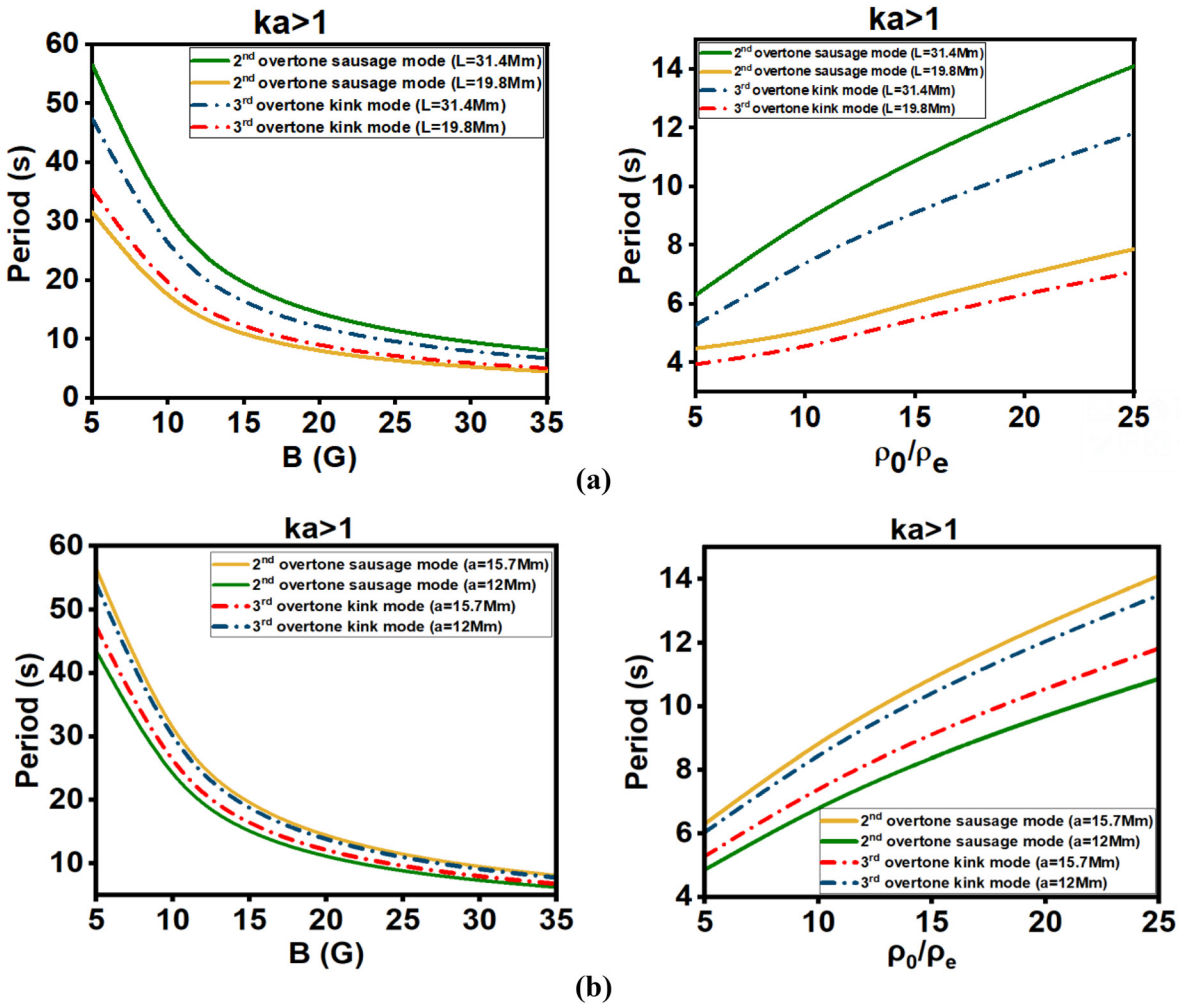

FIG. 5. Variation of period (s) (a) for different length of the loop as a function of magnetic field (G) at $\frac{\rho_0}{\rho_e} = 25$, and as a function of density contrast $\frac{\rho_0}{\rho_e}$ at $B_0 = B_e = 20$ G by keeping the value of radius fixed (i.e., $a = 15.7$ mm) and (b) for different radius of the loop as a function of magnetic field (G) at $\frac{\rho_0}{\rho_e} = 25$, and as a function of density contrast $\frac{\rho_0}{\rho_e}$ at $B_0 = B_e = 20$ G by keeping length of the loop fixed (i.e., $k = 10^{-9}$ cm^{-1}) of leaky second overtone sausage and third overtone kink mode waves at $T_0 = T_e = 10^6$ K, for a different aspect ratio (a/L) of the loop to maintain dimensionless wavenumber, $ka > 1$.

$$\Delta\tau = \left(\frac{\tau_{ideal} - \tau_{non-ideal.}}{\tau_{ideal}}\right) \times 100, \tag{21}$$

where $\Delta\tau$ is variation in damping time, τ_{ideal} is the damping time for ideal plasma, and $\tau_{non-ideal}$ is the damping time for non-ideal plasma.

Figures 7(a) and 7(b) show the variation of damping time as a function of density contrast for the fundamental leaky sausage and first overtone kink mode waves and considering the same aspect ratio (a/L) as used in Fig. 6. It is clear from this figure that a thinner and longer loop exhibits stronger damping as compared to wider and shorter loop and that the damping time increases with higher density contrast. Additionally, damping is more pronounced in non-ideal plasma compared to ideal plasma. Figures 7(c) and 7(d) show the estimated changes in damping time for leaky sausage and kink mode waves in comparison with their values in an ideal plasma, for both long- and short-wavelength limits.

For the fast leaky sausage mode [Fig. 7(c)], in the long-wavelength regime, the damping time in the non-ideal plasma is about 3%–4% lower than in the ideal case as the density contrast increases from 5 to 25, indicating enhanced damping. In the short-wavelength regime, this difference becomes more significant, ranging from approximately 9%–32% over the same range of density contrast. Similarly, for the leaky kink mode [Fig. 7(d)], both the long- and short-wavelength regimes show greater damping in the presence of viscosity. Initially, the damping is around 10% higher than in the ideal case and increases up to about 12% in the long-wavelength limit and 18% in the short-wavelength limit as the density contrast rises from 5 to 25. Like the sausage mode, the damping effect becomes more prominent with higher density contrasts. These results demonstrate that

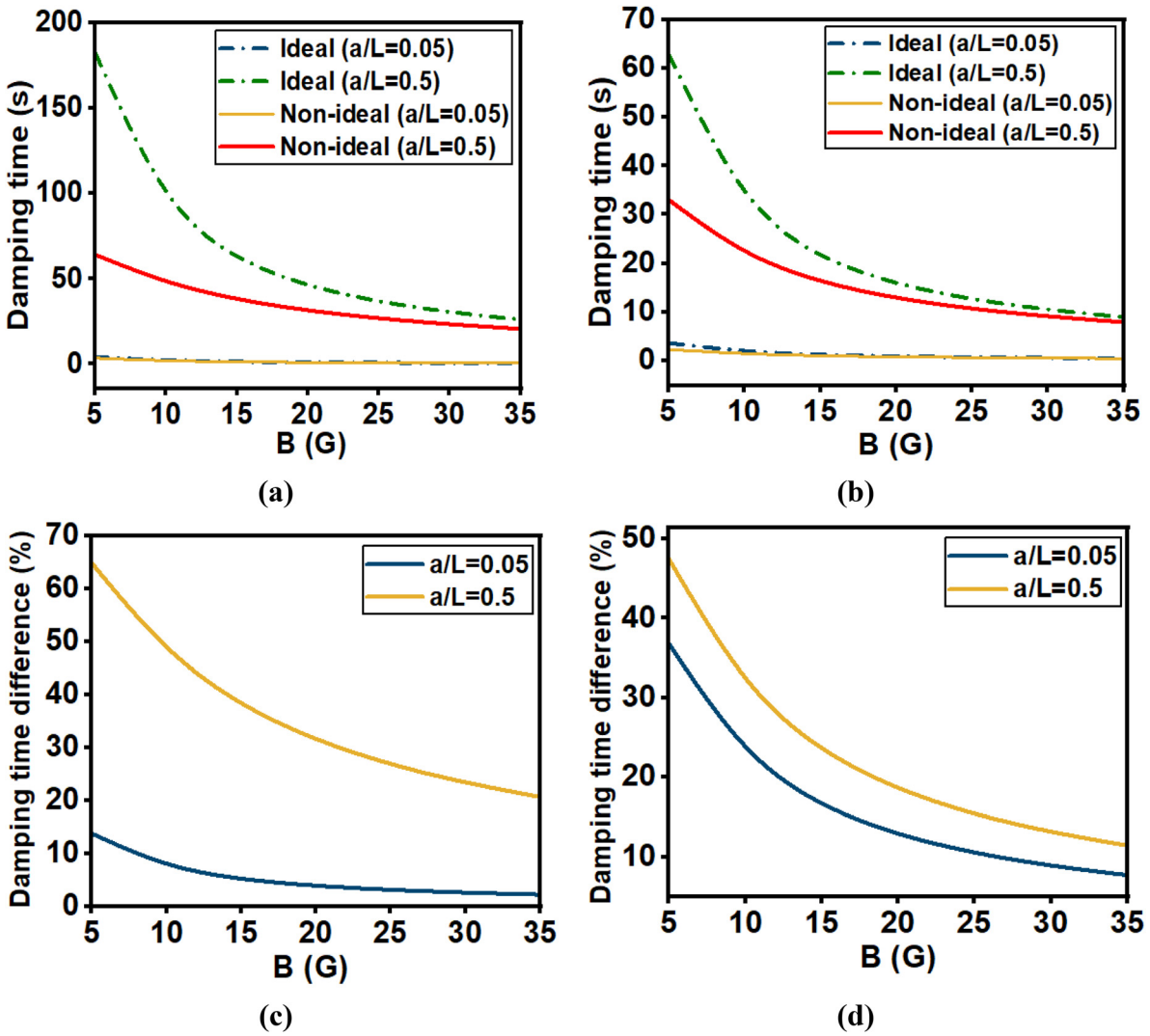

FIG. 6. Variation of damping time (s) as a function of magnetic field (G) for both long ($ka < 1$ or $\frac{a}{L} < 0.3$) and short for ($ka > 1$ or $\frac{a}{L} > 0.3$) wavelength limits for (a) fundamental sausage, (b) first overtone kink mode waves, (c) difference in damping time for sausage, and (d) difference in damping time for kink at $T_0 = T_e = 10^6$ K, $\frac{\rho_0}{\rho_e} = 25$, $k = 10^{-8}$ cm^{-1}, for different values of aspect ratio (a/L).

viscosity has a stronger impact on wave damping at higher density contrasts for both the sausage and kink modes, respectively. A specific mix of physical characteristics is needed to achieve better damping, as shown in Figs. 6 and 7. Specifically, a smaller density contrast and a thin and long loop with a higher magnetic field strength are essential for optimizing the damping effect.

The Q-factor determines the number of oscillations before the wave damp into the considering region and is defined by ratio of damping time to the wave period. The higher value of Q-factor (i.e., $\gg 1$) reflects the weak damping while lower value (≤ 1) of it corresponds to strong damping (Nakariakov and Verwichte, 2005; Pandey and Dwivedi, 2006; Pascoe *et al.*, 2012; Nisticò *et al.*, 2013; and Ruderman and Goossens, 2014). The strength of damping of leaky fundamental sausage and first overtone kink mode (as shown in Figs. 4 and 5) waves in coronal loops, particularly those with step-function radial density profiles, is profoundly influenced by the magnetic field strength, as illustrated in Fig. 8. We have already shown in Fig. 6 that thin and longer loop where waves propagate shows stronger damping, thereby decreasing the Q-factor compared to wider and shorter loops and as we increase the value of magnetic field, the value of Q-factor is also increases for the non-ideal case and constant throughout for the case of ideal plasma. After incorporating the viscosity as a dissipative term, we found comparatively stronger damping as compared to the ideal plasma case and has lesser Q-factor value.

Figures 8(a) and 8(b) depicts how the Q-factor for the leaky fast MHD waves varies with loop width for both ideal and non-ideal plasmas. Notably, a decrease in loop width is associated with a lower Q-factor, suggesting that the wave is more effectively damped with

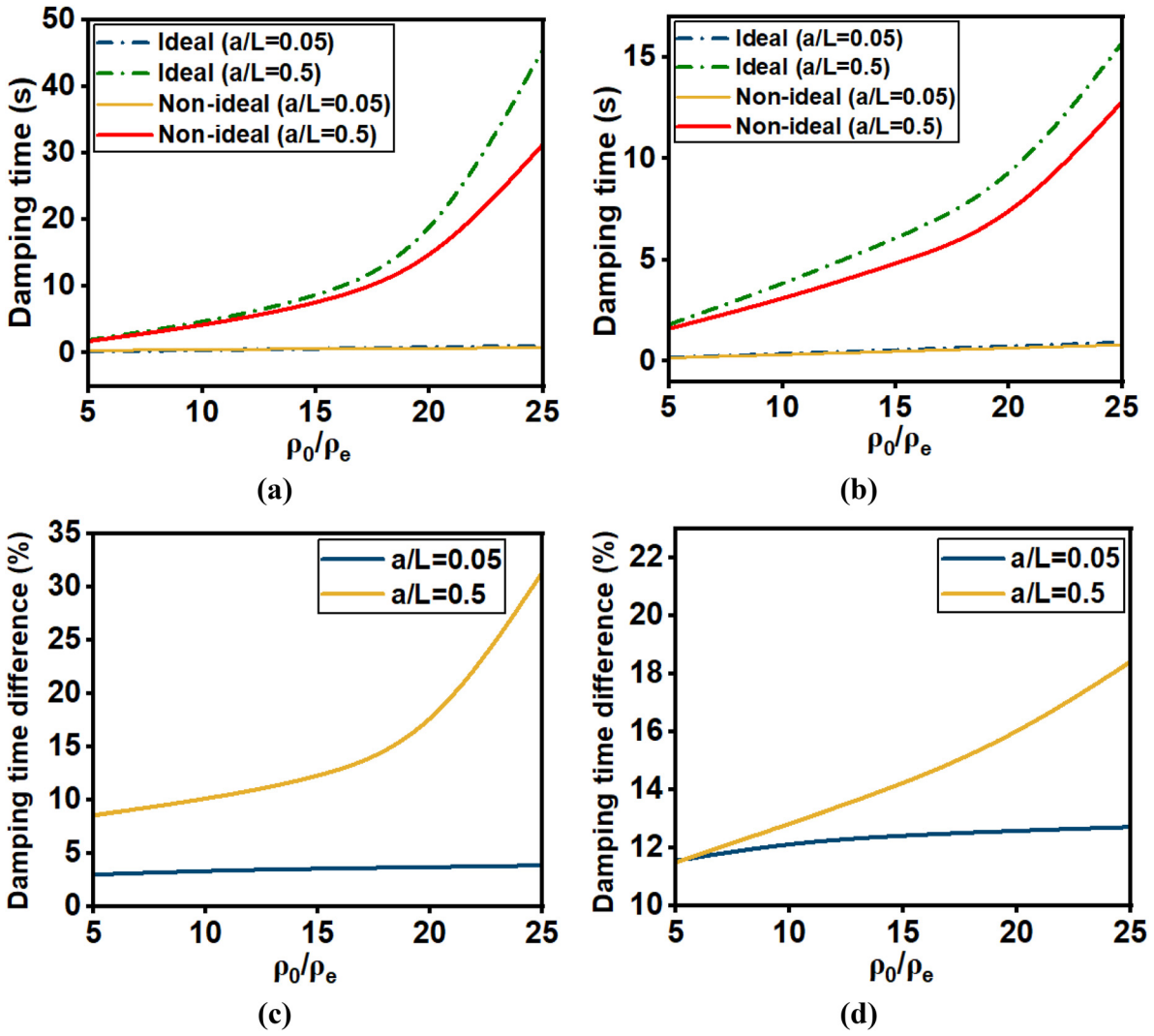

FIG. 7. Variation of damping time (s) as a function of density contrast ρ_0/ρ_e for both long ($ka < 1$ or $\frac{a}{L} < 0.3$) and short for ($ka > 1$ or $\frac{a}{L} > 0.3$) wavelength limits for (a) fundamental sausage, (b) first overtone kink mode waves, (c) difference in damping time for sausage, and (d) difference in damping time for kink at $T_0 = T_e = 10^6$K, $B_0 = B_e = 20$G, $k = 10^{-8}$cm^{-1}, for different values of aspect ratio (a/L),

respect to time. In this situation, the wave releases more energy into the surrounding area. Longer and narrower loops display stronger damping than shorter and broader loops, as demonstrated by both ideal and non-ideal cases. To emphasize the results more clearly, we have included plots showing the variation in the value of Q-factor calculated using Eq. (22), illustrating how much it changes in non-ideal plasma compared to the ideal case for both short- and long-wavelength limits, as shown in Figs. 8(c) and 8(d). For sausage modes, in the short-wavelength limit, the Q-factor is about 15% to 3% lower as the magnetic field increases from 5 to 35G. In the long-wavelength limit, the Q-factor decreases more significantly, ranging from about 65% to 22% lower over the same magnetic field range. For kink modes, the Q-factor reduces by approximately 37% to 7% in the long-wavelength regime and by about 47% to 12% in the short-wavelength regime, as the magnetic field increases from 5 to 35G, compared to the ideal plasma case. These results highlight how viscosity affects wave quality effectively in both long and short-wavelength regimes,

$$\Delta Q = \left(\frac{Q_{ideal} - Q_{non-ideal}}{Q_{ideal}}\right) \times 100, \tag{22}$$

where ΔQ is variation in damping time, Q_{ideal} is the damping time for ideal plasma, and $Q_{non-ideal}$ is the damping time for non-ideal plasma.

In Fig. 9, we illustrate the Q-factor of transverse leaky fast MHD waves with varying density contrast in coronal loops, while maintaining a constant magnetic field. In this figure, we have considered the leaky fundamental sausage and first overtone kink mode waves for plotting it with density contrast, because the higher harmonics modes

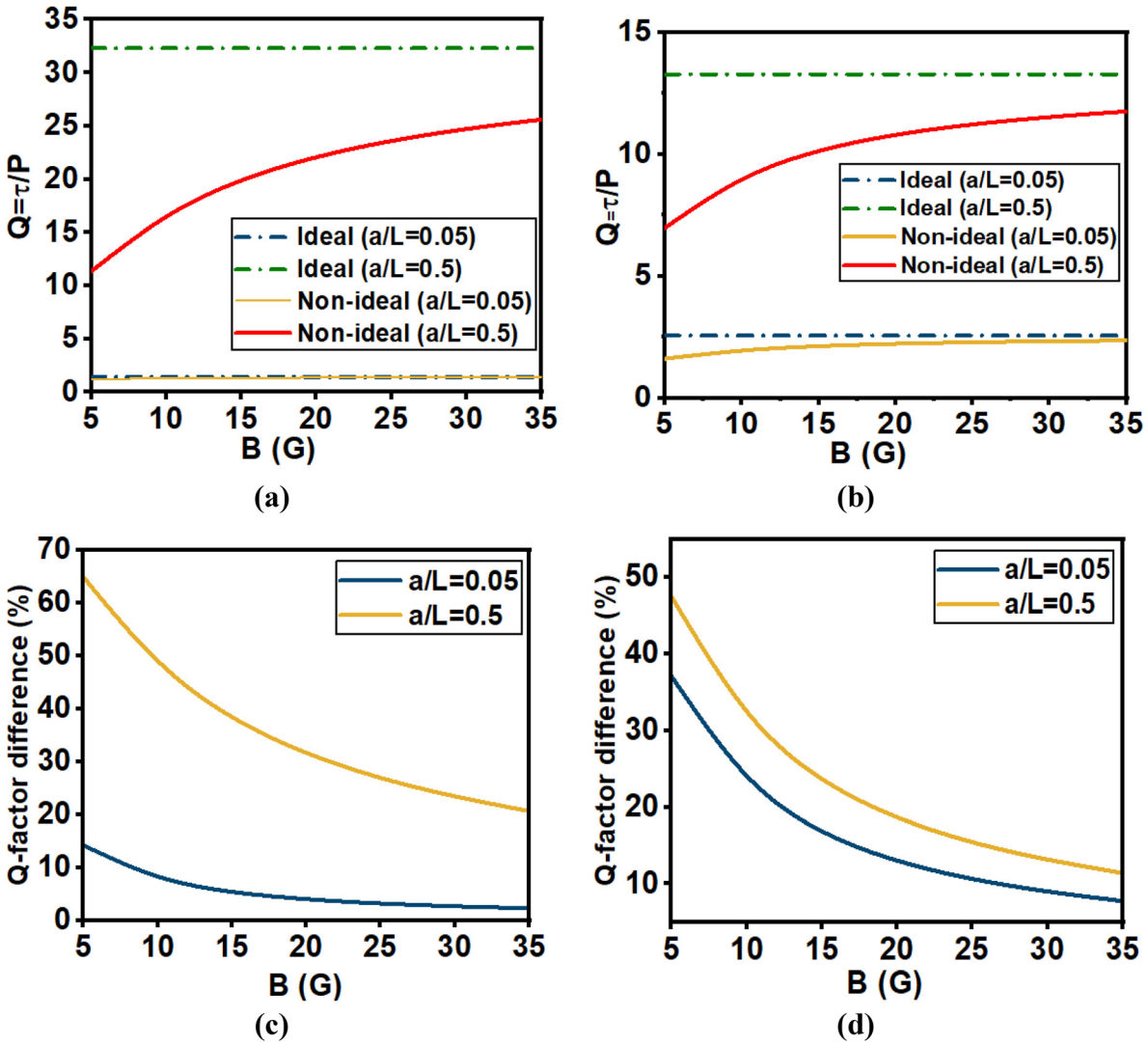

FIG. 8. Variation of Q-factor (i.e., τ/P) as a function of magnetic field (G) for both long ($ka < 1$ or $\frac{a}{L} < 0.3$) and short for ($ka > 1$ or $\frac{a}{L} > 0.3$) wavelength limits for the (a) fundamental sausage, (b) first overtone kink modes, (c) Q-factor difference for sausage, and (d) Q-factor difference for kink at $T_0 = T_e = 10^6$K, $\frac{\rho_0}{\rho_e} = 25$, $k = 10^{-8}$cm^{-1}, for different values of aspect ratio (a/L).

(second and third order) are difficult to detect, and there is no observational support regarding their existence neither for leaky nor for the trapped modes. This depiction mirrors the trend observed in Fig. 8, where a decrease in loop width corresponds to a lower Q-factor across both ideal and non-ideal conditions and shows an increasing behavior with the density contrast. We have shown the behavior of Q-factor as a function of both magnetic field strength and density contrast. It underscores that narrower and larger coronal loops show stronger damping than those with wider and shorter loops. Additionally, in Figs. 9(c) and 9(d)—similar to Figs. 8(c) and 8(d)—the percentage change in the relative value of Q-factor for fast sausage mode waves is about 4%–5% with the increase in density contrast from 5 to 25 in the long-wavelength limit and varies from 9% to 32% with the same density contrast regime in the short-wavelength limit. For fast leaky kink modes, the percentage change in the relative value of the Q-factor is around 12%–13% with a similar density contrast regime for the long wavelength limits and varies from 11% to 18% with same density contrast regime for short wavelength limits. This indicates that both wavelength limits analysis of leaky fast MHD waves contribute to coronal heating and magneto-seismology applications. However, the long-wavelength limit shows stronger damping as compared to short wavelength limit, suggesting long wavelength limit plays a more significant role compared to the short-wavelength approximation.

Plasma viscosity inherently depends on plasma temperature, as shown in Eq. (23). To illustrate this relationship and its effect on wave damping, Tables I and II present the characteristic values of damping

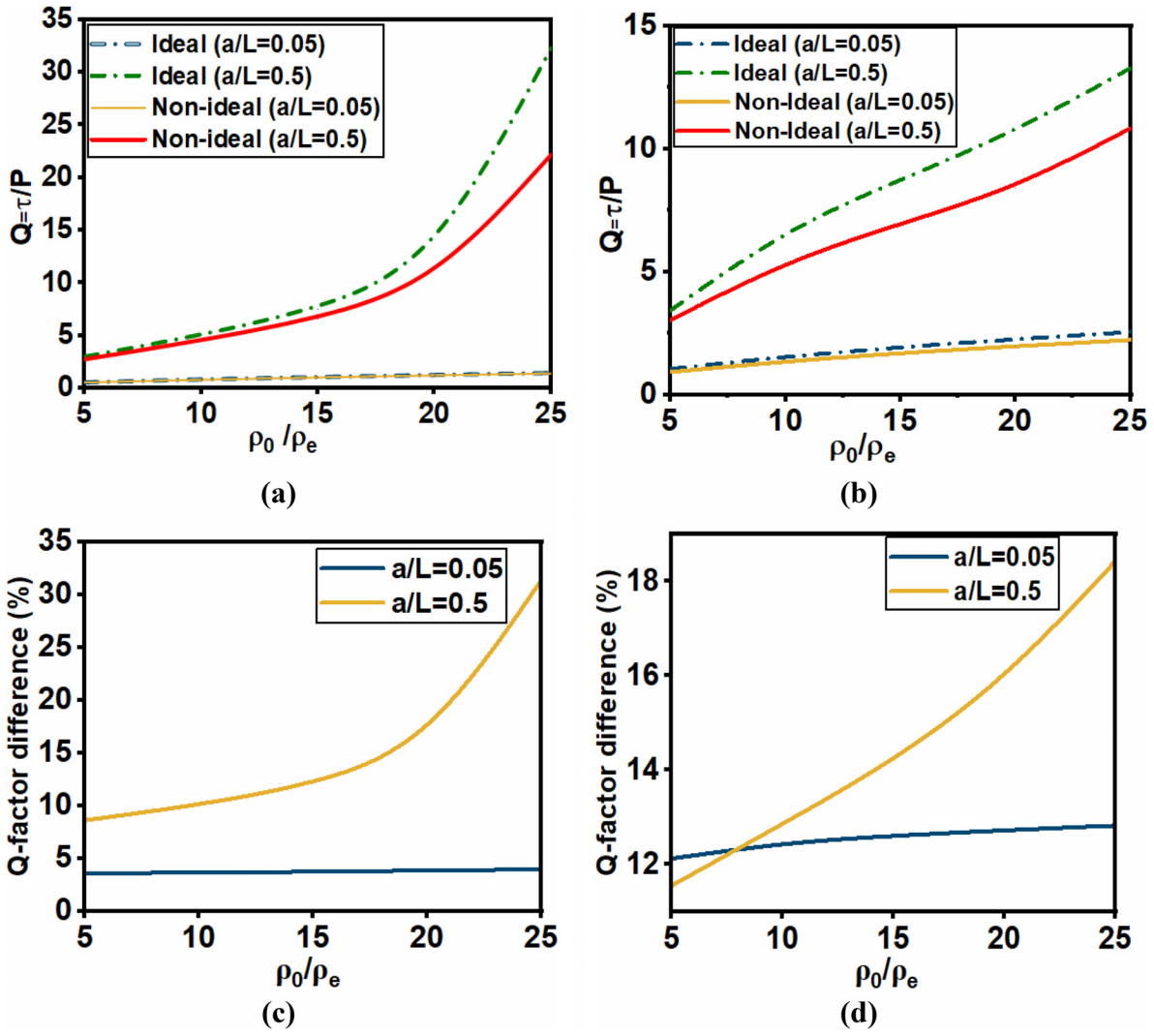

FIG. 9. Variation of Q-factor (i.e., τ/P) as a function of density contrast ρ_0/ρ_e for both long ($ka < 1$ or $\frac{a}{L} < 0.3$) and short for ($ka > 1$ or $\frac{a}{L} > 0.3$) wavelength limits for the (a) fundamental sausage, (b) first overtone kink modes, (c) Q-factor difference for sausage, and (d) Q-factor difference for kink at $T_0 = T_e = 10^6$K, $B_0 = B_e = 20$G, $k = 10^{-8}$cm^{-1}, for different values of the aspect ratio (a/L).

TABLE I. Characteristic values of damping time and Q-factor for leaky sausage mode waves for both long and short wavelength limit.

Temperature (MK)	Viscosity ($gcm^{-1}s^{-1}$)	Damping time (s) for long wavelength limit (a/L = 0.05)	Q-factor for long wavelength limit (a/L = 0.05)	Damping time (s) for short wavelength limit (a/L = 0.5)	Q-factor for short wavelength limit (a/L = 0.5)
1	0.1	0.980 601	1.363 412	31.282 35	22.16
2	0.56	0.832 185	1.150 277	...	...
4	3.2	0.454 401	0.602 023	...	...
6	8.81	0.241 345	0.273 973	...	...
8	18.1	...	...	...	...
10	31.6	...	...	...	...

TABLE II. Characteristic values of damping time and Q-factor for leaky kink mode waves for both long and short wavelength limit.

Temperature (MK)	Viscosity ($gcm^{-1}s^{-1}$)	Damping time (s) for long wavelength limit (a/L = 0.05)	Q-factor for long wavelength limit (a/L = 0.05)	Damping time (s) for short wavelength limit (a/L = 0.5)	Q-factor for short wavelength limit (a/L = 0.5)
1	0.1	0.799 582	2.223 51	12.804 38	10.83
2	0.56	0.503 147	1.389 684	6.894 821	5.83
4	3.2	0.165 736	0.424 135	...	...
6	8.81	0.074 472	0.103 584	...	...
8	18.1	0.019 321	0.023 345	...	...
10	31.6	...	...	...	...

time and quality factor (Q-factor) across a range of viscosities, for both long- and short-wavelength limits of leaky sausage and kink mode waves, respectively. The viscosity is

$$\mu = 10^{-16}\, T^{5/2}\, \mathrm{gcm^{-1}s^{-1}}. \tag{23}$$

It is clear from Table I, as the plasma temperature increases, viscosity is also going to increase. This increase in viscosity leads to a reduction in both damping time and Q-factor, indicating that wave energy dissipates more rapidly for both the long and short wavelength limit. For leaky sausage mode waves in the long-wavelength limit, a cutoff occurs at a viscosity of approximately $18.1\,\mathrm{gcm^{-1}s^{-1}}$, corresponding to a temperature of 8 MK. In the short-wavelength limit, valid values of damping time and Q-factor are obtained only at 1 MK; higher temperatures lead to cutoffs, as the solutions fall outside the interested region.

For leaky kink mode waves, a similar pattern is observed: increasing temperature leads to decreasing damping time and Q-factor. However, unlike the sausage mode, the kink mode yields one additional valid solution in both wavelength regimes. In this case, the cutoffs occur at 10 MK for the long-wavelength limit and 4 MK for the short-wavelength limit.

V. CONCLUSIONS

Our model of coronal loops is analogous to a rectangular magnetic waveguide, containing viscous plasma, thereby viscous wave heating and radiative losses, and support the existence of the leaky fast MHD modes. There are a number of studies on the existence of leaky modes concerning the topic of patch antennas design and developments in the realms of electromagnetic radiation in free space (e.g., Monticone and Alu, 2015; Tofani and Fuscaldo, 2020; Zheng *et al.*, 2023; and Menon *et al.*, 2023). Motivated with this idea of leaky modes, in this work, we have studied the characterization of transverse fast MHD leaky waves in coronal loops wherein radiation is taking place away from the considered loop. The density contrast in the loop is considered with step-function radial density profiles such as $\frac{\rho_0}{\rho_e} = constant$. We employed a low-$\beta$ plasma with 1-D perturbation in velocity $[V_{1x}, 0, 0]$, the perturbation in velocity is independent of the y-variable $\left(\frac{\partial}{\partial y} = 0\right)$, while perturbation in velocity along z-direction is neglected due to low-β assumption ($V_{1z} \ll V_{1x}$ and V_{1y}) (Porter *et al.*, 1994; Wang, 2011; Wang *et al.*, 2021; and Pandey *et al.*, 2022b). This simplification retains the essential physics of wave propagation in the solar corona. Previous studies have shown that such structured regions support both trapped (Edwin and Roberts, 1982) and leaky mode waves (Terradas *et al.*, 2005) in ideal plasmas. For non-ideal plasma, study on trapped modes has been performed by Porter *et al.* (1994); Pandey *et al.* (2022b) for rectangular geometry, but for the leaky mode, a detailed examination is yet to be considered.

In what follows, we derived a general analytical dispersion relation for fast leaky MHD waves, where wave leakage is allowed from the waveguide, which is different from the existing formulation of the trapped mode waves in dissipative medium as reported previously by Porter *et al.* (1994) and further followed by Pandey *et al.* (2022b) within the slab geometry of coronal loops. We have calculated the period and damping time for the fast leaky transverse sausage and kink mode waves in the presence of dissipative term (i.e., viscosity). For this, we have studied the characteristics of transverse leaky waves in coronal loops, with the variation of magnetic field strength and density contrast under the assumption of long wavelength and short wavelength approximation (i.e., $ka < 1$ and $ka > 1$). For $ka < 1$, the period of fast leaky waves varies primarily with the loop width and shows decreasing and increasing behavior with respect to the increase value of magnetic field and density contrast respectively, as shown in Fig. 4. Interestingly, changing the loop length in this regime does not significantly affect the wave periods (Spruit, 1982; Cally, 1986).

However, in the case of $ka > 1$ (Fig. 5), the periods of fast leaky sausage and kink mode waves are influenced by both the loop width and length of the loop and shows the decreasing pattern with magnetic field and increasing pattern with variation of density contrast (Spruit, 1982; Cally, 1986). In leaky mode, longer and narrower loops show stronger damping in the case of ideal plasma. Furthermore, introducing viscosity as a dissipative term further complicates this picture. In the presence of viscosity, waves exhibit even stronger damping as compared to ideal plasma as shown in Figs. 6 and 7, particularly in longer and narrower loops ($ka < 1$) than shorter and wider loops ($ka > 1$). Additionally, we may state that the effect of viscosity on the percentage change in the value of damping time of leaky modes is significant, as shown in Figs. 7(c), 7(d), 8(c), and 8(d). Apart from this, the proposed approach can also be used for the coronal magneto-seismological applications. In our study, the calculated period could be explained by specific loop lengths, particularly those around 1–10 mm, commonly observed in coronal bright points (CBPs) (Golub *et al.*, 1977; Hirzberger *et al.*, 2008; and Mou *et al.*, 2018). This range of loop sizes provides a suitable framework for interpreting our results in both the long and short wavelength limits. Particularly, in the case of the short wavelength limit, period corresponding to the second and third overtones have yet to be observed. However, with advancements in

observational capabilities in the future, we anticipate that these higher harmonics may be detected. Our theoretical model may be supplementary work for them.

Leaky modes may play a crucial role in loop dynamics and are important from an energy perspective. The defects identified by Goedbloed *et al.* (2023) in the standard leaky mode model are valid, and their corresponding solutions provide crucial insights for improving the model when one is interested in its spatial evolution. We have adopted a step density profile to study fast leaky mode waves, a concept that similar to quantum potential wells approach, where a Schrödinger wave function is confined by potential energy barriers when its strength is infinite. However, if the strength of boundaries is finite, quantum tunneling effects allow the wavefunction to leak from the structure in form of propagating wave. The method for finding the solution for our differential equation (20) using step type density profile is analogous to quantum approach, emphasizing the principles of wave behavior across different domains (Sakurai *et al.*, 1986; Griffiths, 1995; and Zettili, 2001). Additionally, exponential growth in solutions at infinity is typically observed in models with continuous driver source where frequency is specified and dispersion relation is solved for complex waves number k. However, in this study, we solved the dispersion relation for complex frequency by specified the wavenumber k real and fixed. As a result, we are calculating damping time ($\frac{1}{Im(\omega)}$), instead of damping length. Our analysis has been focused on low-β plasma conditions, where the slow mode waves corresponding to longitudinal perturbations do not significantly alter the results. In this study, we did not take into account the influence of the kinetic pressure (i.e., finite plasma-β), which determines the inclusion of slow mode waves in the system, nor did we address the asymmetry of the system. These factors may significantly affect the damping characteristics of the waves. We intend to investigate these aspects in our future research efforts.

ACKNOWLEDGMENTS

V.S. Pandey acknowledges the Science and Engineering Research Board-Department of Science and Technology, Core Research Grant (SERB-DST, CRG) Project, Grant No. CRG/2022/007017.

R.E. acknowledges the NKFIH (OTKA, Grant No. K142987) Hungary for enabling this research. R.E. is also grateful to Science and Technology Facilities Council (STFC, Grant No. ST/M000826/1) UK, PIFI (China, Grant No. 2024PVA0043) and the NKFIH Excellence Grant No. TKP2021-NKTA-64 (Hungary).

AUTHOR DECLARATIONS

Conflict of Interest

The authors have no conflicts to disclose.

Author Contributions

Ankit Kumar: Conceptualization (equal); Formal analysis (equal); Methodology (equal); Writing – original draft (equal); Writing – review & editing (equal). **V. S. Pandey:** Funding acquisition (equal); Supervision (equal); Writing – review & editing (equal). **Sweta Singh:** Formal analysis (equal); Methodology (equal). **Preeti Verma:** Writing – review & editing (equal). **R. Erdelyi:** Writing – review & editing (equal).

DATA AVAILABILITY

The data that support the findings of this study are available from the corresponding author upon reasonable request.

REFERENCES

Allcock, M. and Erdélyi, R., "Magnetohydrodynamic waves in an asymmetric magnetic slab," Sol. Phys. **292**(2), 35 (2017).

Allcock, M., Shukhobodskaia, D., Zsámberger, N. K., and Erdélyi, R., "Magnetohydrodynamic waves in multi-layered asymmetric waveguides: Solar magneto-seismology theory and application," Front. Astron. Space Sci. **6**, 48 (2019).

Allian, F. and Jain, R., "The need for new techniques to identify the high-frequency MHD waves of an oscillating coronal loop," Astron. Astrophys. **650**, A91 (2021).

Andries, J., Van Doorsselaere, T., Roberts, B., Verth, G., Verwichte, E., and Erdélyi, R., "Coronal seismology by means of kink oscillation overtones," Space Sci. Rev. **149**, 3–29 (2009).

Antia, D. D., "Kinetic method for modeling vitrinite reflectance," Geology **14**(7), 606–608 (1986).

Arregui, I., "Wave heating of the solar atmosphere," Philos. Trans. R. Soc. A **373**(2042), 20140261 (2015).

Arregui, I., Oliver, R., and Ballester, J. L., "Prominence oscillations," Living Rev. Sol. Phys. **15**(1), 3 (2018).

Aschwanden, M. J., Fletcher, L., Schrijver, C. J., and Alexander, D., "Coronal loop oscillations observed with the transition region and coronal explorer," Astrophys. J. **520**(2), 880 (1999).

Aschwanden, M. J., De Pontieu, B., Schrijver, C. J., and Title, A. M., "Transverse oscillations in coronal loops observed with TRACE–II. Measurements of geometric and physical parameters," Sol. Phys. **206**, 99–132 (2002).

Brady, C. S., Verwichte, E., and Arber, T. D., "Leakage of waves from coronal loops by wave tunneling," Astron. Astrophys. **449**(1), 389–399 (2006).

Braginskii, S. I. and Leontovich, M. A., *Reviews of Plasma Physics*, edited by A. M. A. Leontovich (Consultants Bureau, 1965), pp. 205–311.

Bray, R. J., Cram, L. E., Durrant, C. J., and Loughhead, R. E., *Plasma Loops in the Solar Corona*, Cambridge Astrophysics Series 18 (Cambridge University Press, 1991).

Cally, P. S., "Leaky and non-leaky oscillations in magnetic flux tubes," Sol. Phys. **103**, 277–298 (1986).

Cally, P. S., "Coronal leaky tube waves and oscillations observed with trace," Sol. Phys. **217**, 95–108 (2003).

Cally, P. S., "Note on the initial value problem for coronal loop kink waves," Sol. Phys. **233**, 79–87 (2006).

Chen, S. X., Li, B., Guo, M., Shi, M., and Yu, H., "Oblique quasi-kink modes in solar coronal slabs embedded in an asymmetric magnetic environment: Resonant damping, phase and group diagrams," Astrophys. J. **940**(2), 157 (2022).

De Moortel, I. and Nakariakov, V. M., "Magnetohydrodynamic waves and coronal seismology: An overview of recent results," Philos. Trans. R. Soc. A **370**(1970), 3193–3216 (2012).

De Moortel, I., Pascoe, D. J., Wright, A. N., and Hood, A. W., "Transverse, propagating velocity perturbations in solar coronal loops," Plasma Phys. Controlled Fusion **58**(1), 014001 (2016).

Díaz, A. J., Zaqarashvili, T., and Roberts, B., "Fast magnetohydrodynamic oscillations in a force-free line-tied coronal arcade," Astron. Astrophys. **455**(2), 709–717 (2006).

Ebrahimi, Z., "On the sausage magnetohydrodynamic waves in magnetic flux tubes: Finite plasma beta and phase mixing," Mon. Not. R. Astron. Soc. **534**(3), 1928–1936 (2024).

Edwin, P. M. and Roberts, B., "Wave propagation in a magnetically structured atmosphere. III: The slab in a magnetic environment," Sol. Phys. **76**, 239–259 (1982).

Edwin, P. M. and Roberts, B., "Wave propagation in a magnetic cylinder," Sol. Phys. **88**, 179–191 (1983).

Edwin, P. M. and Roberts, B., "Employing analogies for ducted MHD waves in dense coronal structures," Astron. Astrophys. **192**(1–2), 343–347 (1988).

Einaudi, G., Chiuderi, C., and Califano, F., "Coronal heating and solar activity: The role of waves," Adv. Space Res. **13**(9), 85–94 (1993).

Erdélyi, R. and Ballai, I., "Heating of the solar and stellar coronae: A review," Astron. Nachr. **328**(8), 726–733 (2007).
Erdélyi, R. and Goossens, M., "Resonant absorption of Alfvén waves in coronal loops in visco-resistive MHD," Astron. Astrophys. **294**(2), 575–586 (1995).
Erdélyi, R. and Goossens, M., "Effects of flow on resonant absorption of MHD waves in viscous MHD," Astron. Astrophys. **313**, 664–673 (1996).
Erdélyi, R. and Zsámberger, N. K., "Magnetohydrodynamic waves in asymmetric waveguides and their applications in solar physics—A review," Symmetry **16**(9), 1228 (2024).
Farahani, S. V., Hornsey, C., Van Doorsselaere, T., and Goossens, M., "Frequency and damping rate of fast sausage waves," Astrophys. J. **781**(2), 92 (2014).
Gizon, L. and Birch, A. C., "Local helioseismology," Living Rev. Sol. Phys. **2**, 1–131 (2005).
Goedbloed, H., Keppens, R., and Poedts, S., "Leaky modes in coronal magnetic flux tubes revisited," J. Plasma Phys. **89**(5), 905890520 (2023).
Golub, L., Krieger, A. S., Harvey, J. W., and Vaiana, G. S., "Magnetic properties of X-ray bright points," Sol. Phys. **53**, 111–121 (1977).
Gordon, B. E. and Hollweg, J. V., "Collisional damping of surface waves in the solar corona," Astrophys. J. **266**, 373–382 (1983).
Gough, D. O., Kosovichev, A. G., Toomre, J., Anderson, E., Antia, H. M., Basu, S. *et al.*, "The seismic structure of the Sun," Science **272**(5266), 1296–1300 (1996).
Griffiths, D., *Introduction to Elementary Particles* (John Wiley & Sons, 1995).
Hirzberger, J., Gizon, L., Solanki, S. K., and Duvall, T. L., "Structure and evolution of supergranulation from local helioseismology," Sol. Phys. **251**, 417–437 (2008).
Hollweg, J. V., "Viscosity and the Chew-Goldberger-Low equations in the solar corona," Astrophys. J. **306**, 730–739 (1986).
Hornsey, C., Nakariakov, V. M., and Fludra, A., "Sausage oscillations of coronal plasma slabs," Astron. Astrophys. **567**, A24 (2014).
Howson, T. A., De Moortel, I., and Reid, J., "Phase mixing and wave heating in a complex coronal plasma," Astron. Astrophys. **636**, A40 (2020).
Kolotkov, D. Y., Duckenfield, T. J., and Nakariakov, V. M., "Seismological constraints on the solar coronal heating function," Astron. Astrophys. **644**, A33 (2020).
Kumar, A. and Pandey, V. S., "High-frequency dissipative MHD waves in straight magnetic cylindrical plasma: Coronal loops heating application," Phys. Plasmas **31**(2), 022109 (2024).
Li, B., Antolin, P., Guo, M. Z., Kuznetsov, A. A., Pascoe, D. J., Van Doorsselaere, T., and Vasheghani Farahani, S., "Magnetohydrodynamic fast sausage waves in the solar corona," Space Sci. Rev. **216**, 1–42 (2020).
Lopin, I., "Kink oscillations in a coronal loop arcade with finite plasma-β: Effect of oblique propagation," Mon. Not. R. Astron. Soc. **514**(3), 4329–4342 (2022).
Lopin, I. and Nagorny, I., "Fast waves in a smooth coronal slab," Astrophys. J. **801**(1), 23 (2015).
Marquardt, D. W., "An algorithm for least-squares estimation of nonlinear parameters," J. Soc. Ind. Appl. Math. **11**(2), 431–441 (1963).
Martín-Palma, R. J., "Quantum tunneling in low-dimensional semiconductors mediated by virtual photons," AIP Adv. **10**(1), 015145 (2020).
Mathioudakis, M., Jess, D. B., and Erdelyi, R., "Alfvén waves in the solar atmosphere: From theory to observations," Space Sci. Rev. **175**, 1–27 (2013).
Menon, S. S., Kalra, S., Pathak, S. K., Sivanandan, N., and Hariharan, S. M., "Leaky mode analysis of solid dielectric horn antenna," Prog. Electromagn. Res. M **121**, 95–106 (2023).
Monticone, F. and Alu, A., "Leaky-wave theory, techniques, and applications: From microwaves to visible frequencies," Proc. IEEE **103**(5), 793–821 (2015).
Moré, J. J., "The Levenberg-Marquardt algorithm: Implementation and theory," in *Numerical Analysis: Proceedings of the Biennial Conference, Dundee, Scotland, June 28–July 1* (Springer, Berlin, Heidelberg, 1977), pp. 105–116.
Moré, J. J., Garbow, B. S., and Hillstrom, K. E., *User Guide for MINPACK-1* (Argonne National Laboratory, Argonne, IL, 1980).
Morton, R. J., Verth, G., Jess, D. B., Kuridze, D., Ruderman, M. S., Mathioudakis, M., and Erdélyi, R., "Observations of ubiquitous compressive waves in the Sun's chromosphere," Nat. Commun. **3**(1), 1315 (2012).
Mou, C., Madjarska, M. S., Galsgaard, K., and Xia, L., "Eruptions from quiet Sun coronal bright points. I. Observations," Astron. Astrophys. **619**, A55 (2018).
Nakariakov, V. M., Anfinogentov, S. A., Antolin, P., Jain, R., Kolotkov, D. Y., Kupriyanova, E. G. *et al.*, "Kink oscillations of coronal loops," Space Sci. Rev. **217**(6), 73 (2021).
Nakariakov, V. M. and Verwichte, E., "Coronal waves and oscillations," Living Rev. Sol. Phys. **2**(1), 3 (2005).
Nisticò, G., Nakariakov, V. M., and Verwichte, E., "Decaying and decayless transverse oscillations of a coronal loop," Astron. Astrophys. **552**, A57 (2013).
Ofman, L., Davila, J. M., and Steinolfson, R. S., "Coronal heating by the resonant absorption of Alfven waves: The effect of viscous stress tensor," Astrophys. J. **421**(1), 360–371 (1994).
Ofman, L. and Wang, T., "Excitation and damping of slow magnetosonic waves in flaring hot coronal loops: Effects of compressive viscosity," Astrophys. J. **926**(1), 64 (2022).
Pandey, V. S. and Dwivedi, B. N., "Strong and weak damping of slow MHD standing waves in hot coronal loops," Sol. Phys. **236**, 127–136 (2006).
Pandey, V. S., Kumar, A., and Nayak, M. K., "Transverse oscillations of the incompressible MHD mode in the visco-resistive plasmas: An explanation of Alfvénic to Landau-type characteristics," Mon. Not. R. Astron. Soc. **511**(1), 1349–1361 (2022a).
Pandey, V. S., Kumar, A., and Nayak, M. K., "The role of linearly polarized transverse MHD waves in heating the solar coronal plasma," Mon. Not. R. Astron. Soc. **513**(3), 3372–3386 (2022b).
Pascoe, D. J., Hood, A. W., De Moortel, I., and Wright, A. N., "Spatial damping of propagating kink waves due to mode coupling," Astron. Astrophys. **539**, A37 (2012).
Pascoe, D. J., Wright, A. N., De Moortel, I., and Hood, A. W., "Excitation and damping of broadband kink waves in the solar corona," Astron. Astrophys. **578**, A99 (2015).
Porter, L. J., Klimchuk, J. A., and Sturrock, P. A., "The possible role of high-frequency waves in heating solar coronal loops," Astrophys. J. **435**(1), 502–514 (1994).
Powell, M. J., "A Fortran subroutine for solving systems of nonlinear algebraic equations," Report No. AERE-R-5947 (Atomic Energy Research Establishment, Harwell, United Kingdom, 1968).
Roberts, B., *MHD Waves in the Solar Atmosphere* (Cambridge University Press, 2019).
Ruderman, M. S. and Roberts, B., "Leaky and non-leaky kink oscillations of magnetic flux tubes," J. Plasma Phys. **72**(3), 285–308 (2006).
Ruderman, M. S. and Goossens, M., "Nonlinear kink oscillations of coronal magnetic loops," Sol. Phys. **289**, 1999–2020 (2014).
Russell, A. J., "Nonlinear damping and field-aligned flows of propagating shear Alfvén waves with Braginskii viscosity," Astrophys. J. **948**(2), 128 (2023).
Sakurai, J. J., Fu Tuan, S., and Newton, R. G., "Modern quantum mechanics," Am. J. Phys. **54**(7), 668 (1986).
Schrijver, C. J., Aschwanden, M. J., and Title, A. M., "Transverse oscillations in coronal loops observed with TRACE–I. An overview of events, movies, and a discussion of common properties and required conditions," Sol. Phys. **206**, 69–98 (2002).
Shao, Z. A., Porod, W., and Lent, C. S., "Transmission resonances and zeros in quantum waveguide systems with attached resonators," Phys. Rev. B **49**(11), 7453 (1994).
Shrivastav, A. K., Pant, V., Berghmans, D., Zhukov, A. N., Van Doorsselaere, T., Petrova, E., Banerjee, D., Lim, D., and Verbeeck, C., "Statistical investigation of decayless oscillations in small-scale coronal loops observed by Solar Orbiter/EUI," Astron. Astrophys. **685**, A36 (2024).
Spruit, H. C., "Propagation speeds and acoustic damping of waves in magnetic flux tubes," Solar Phys. **75**(1), 3–17 (1982).
Terradas, J., Oliver, R., and Ballester, J. L., "On the excitation of trapped and leaky modes in coronal slabs," Astron. Astrophys. **441**(1), 371–378 (2005).
Tofani, S. and Fuscaldo, W., "Fabry-Perot cavity leaky wave antennas with tunable features for terahertz applications," Condens. Matter **5**(1), 11 (2020).
Tomczyk, S., McIntosh, S. W., Keil, S. L., Judge, P. G., Schad, T., Seeley, D. H., and Edmondson, J., "Alfvén waves in the solar corona," Science **317**(5842), 1192–1196 (2007).
Verwichte, E., Foullon, C., and Nakariakov, V. M., "Fast magnetoacoustic waves in curved coronal loops. I. Trapped and leaky modes," Astron. Astrophys. **446**(3), 1139–1149 (2006).
Verwichte, E., Nakariakov, V. M., and Cooper, F. C., "Transverse waves in a post-flare supra-arcade," Astron. Astrophys. **430**(3), L65–L68 (2005).

Wang, T., "Standing slow-mode waves in hot coronal loops: Observations, modeling, and coronal seismology," Space Sci. Rev. **158**, 397–419 (2011).
Wang, T., Ofman, L., Yuan, D., Reale, F., Kolotkov, D. Y., and Srivastava, A. K., "Slow-mode magnetoacoustic waves in coronal loops," Space Sci. Rev. **217**, 1–55 (2021).
Williams, D. R., Phillips, K. J. H., Rudawy, P., Mathioudakis, M., Gallagher, P. T., O'Shea, E., Keenan, F. P., Read, P., and Rompolt, B., "High-frequency oscillations in a solar active region coronal loop," Mon. Not. R. Astron. Soc. **326**(2), 428–436 (2001).
Yu, D. J., "Dissipative instability of magnetohydrodynamic sausage waves in a compressional cylindrical plasma: Effect of flow shear and viscosity shear," Astrophys. J. **954**(2), 217 (2023).
Yu, H., Li, B., Chen, S. X., and Guo, M. Z., "Kink and sausage modes in nonuniform magnetic slabs with continuous transverse density distributions," Astrophys. J. **814**(1), 60 (2015).
Zettili, N., *Quantum Mechanics: Concepts and Applications* (Wiley, 2001).
Zheng, D., Chan, C. H., and Wu, K., "Leaky-wave structures and techniques for integrated front-end antenna systems," IEEE J. Microwave **3**(1), 368–397 (2023).
Zhong, S., Nakariakov, V. M., Miao, Y., Fu, L., and Yuan, D., "30-min decayless kink oscillations in a very long bundle of solar coronal plasma loops," Sci. Rep. **13**(1), 12963 (2023).